Original Article

Ultrastructural Studies of Acrosomal Formation in the Testis of Male Greater Cane Rat (*Thryonomys swinderianus*)

A. O. Adebayo, A. K. Akinloye, A. O. Ihunwo[1], V. O. Taiwo[2], B. O. Oke[3]

Department of Veterinary Anatomy, College of Veterinary Medicine, Federal University of Agriculture, Abeokuta, Departments of [2]Veterinary Pathology and [3]Veterinary Anatomy, Faculty of Veterinary Medicine, University of Ibadan, Ibadan, Nigeria, [1]School of Anatomical Sciences, Faculty of Health Sciences, University of the Witwatersrand, Johannesburg, South Africa

Abstract

Purpose: In furthering the understanding of the process of spermatogenesis in the greater cane rat, this study describes the ultrastructural spermiogenic transformation and acrosomal formation in the testes of this hystricomorphic rodent that is currently undergoing domestication in parts of West Africa. **Materials and Methods:** Testicular samples were obtained from ten sexually mature cane rats that were perfused-fixed using Karnovsky's fixative (phosphate buffered 2% paraformaldehyde – 2.5% glutaraldehyde fixative at pH 7.4). The samples were processed for ultrastructural analysis and examined under the transmission electron microscope. **Results:** The testes of the cane rat showed uniqueness in its cellular associations and the ultrastructure of the spermatogenic cells especially in the formation of the acrosome. The spermatid differentiation and acrosomal formation occurred in 12 steps with the first three steps being the *Golgi* phase and the next three steps making up the *cap* phase. While the three steps that follow constitute the *acrosomal* phase, the last 3 steps make up the *maturation* phase. At the cap and acrosomal phases, the entire acrosomal system comprising the vesicle and granule covers the head of the spermatids with no clear indentation of the nuclear surface by the formed acrosome. Furthermore, elongated spermatids at the maturation phase contained abundance of nuclear vacuoles. **Conclusion:** This work has not only provided information that will further the understanding of spermatogenesis but also aid the understanding of acrosomal reaction in the reproduction of the greater cane rat.

Keywords: Acrosome, greater cane rat, spermatogenesis, ultrastructure

Introduction

The knowledge of spermatogenesis, especially in male wildlife, is important for protection against extinction. It is also necessary for the improvement of species management as well as to boost male reproductive capacity in natural and artificial breeding programs particularly in those that are currently undergoing domestication and captive-rearing.[1,2]

In all mammalian species, spermatogenesis is a highly synchronized and well-regulated process which entails the transformation of spermatogonia into mature spermatozoa.[3] The cyclic spermatogenic events create defined associations among the differentiating germ cells; spermatogonia, spermatocytes, and spermatids. These associations, commonly referred to as the stages of spermatogenesis, vary from one species to another.[4] Thus, the characterization of the spermatogenic stages in a given species is fundamental to the determination of the duration of the cycle of the seminiferous epithelium as well as the spermatogenic efficiency of that species. According to Segatelli *et al*.,[5] and Costa *et al*.,[2] although the testicular structural architecture may be similar in all mammalian species, morphological differentiation of the spermatids which often follows species specific pattern is the major criteria for classifying the cycle of the seminiferous epithelium into stages.

Ultrastructural studies that describe the transformation of the different organelles and the formation of the acrosomal system in the specialization of the spermatid had been carried out in a number of laboratory and domesticated mammals.[2,6-9]

Access this article online

Quick Response Code:

Website: http://www.jmau.org/

DOI: 10.4103/JMAU.JMAU_28_18

Address for correspondence: Dr. A. O. Adebayo, Department of Veterinary Anatomy, Federal University of Agriculture, P.M.B 2240, Abeokuta, Nigeria.
E-mail: releadebayo@yahoo.com

How to cite this article: Adebayo AO, Akinloye AK, Ihunwo AO, Taiwo VO, Oke BO. Ultrastructural studies of acrosomal formation in the testis of male greater cane rat (*Thryonomys swinderianus*). J Microsc Ultrastruct 2019;7:14-8.

There is scarcity of such studies in wild males especially those undergoing domestication.

The greater cane rat (*Thryonomys swinderianus*) is a hystricomorphic wild rodent found only in Africa. In the West Africa subregion, it is vigorously hunted and exploited for food because of its excellent meat taste and high nutritive value.[10] Giving its level of exploitation, efforts, and resources are now being deployed to its domestication and captive-rearing in this part of Africa with focus on enhancing its male reproductive capacity. Along with providing information on spermatogenesis, this work describes the ultrastructural spermatogenic transformation and acrosomal formation in the testes of the greater cane rat.

Materials and Methods

Animals

Ten captive-reared, sexually mature male greater cane rats, with known reproductive and medical records were used in this work. All the animals had brownish perineal staining which is usually used as index of sexual maturity in the male cane rat.[11] The animals were fed commercial cane rat feed while elephant grass and water were given *ad libitum*. The experimental protocol followed the ethical principles in animal research adopted by the University of Ibadan Animal Ethics and Experimentation Committee.

Sample collection

Each animal was weighed, anesthetized and dissected open after being perfuse-fixed transcardially using the Karnovsky's fixative which is phosphate buffered 2% paraformaldehyde – 2.5% glutaraldehyde fixative at pH 7.4. After opening the abdominal and pelvic cavities, the testes were then dissected out and samples taken for electron microscopy.

Tissue processing for electron microscopy

The samples of each testis were further fixed in the Karnovsky's fixative, postfixed in 1% osmium tetroxide for 1 h, dehydrated in an increasing ethanol series, infiltrated and embedded in Epon-Araldite resin. Semi-thin and Ultrathin sections were cut with an Ultracut S ultramicrotome (Reichert-Jung, Austria). While the semi-thin sections were stained with Toluidine blue-Pyronin Y mixture and examined under Axioskop 2 plus, Carl Zeiss light microscope (Germany), the ultrathin sections were mounted on copper grids, double-contrasted with uranyl acetate and lead citrate and observed in a Phillips CM10 transmission electron microscope.

Results

The testis of the greater cane rat showed normal histoarchitecture with the presence of seminiferous tubules having germinal epithelium that was composed of concentric layers of spermatogonia, spermatocytes, and spermatids together with Sertoli cells [Figure 1]. However, the transformation of the spermatids into spermatozoa which involves the development of the acrosomal system and changes in the nuclear

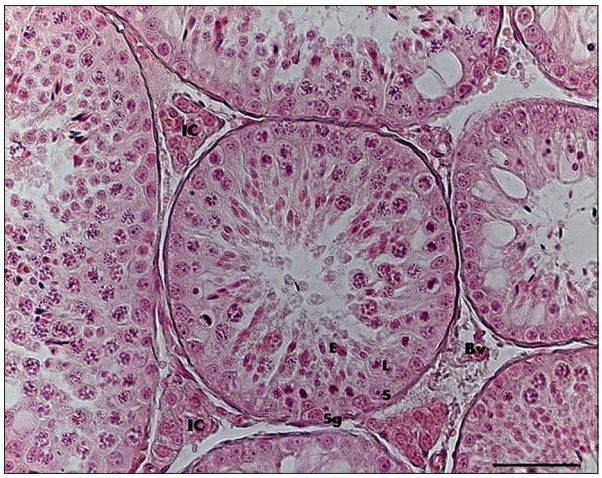

Figure 1: Seminiferous tubule of the greater cane rat showing Sertoli cells (S), spermatogonia (Sg), spermatocytes (L) and elongated spermatids (E). Note the interstitial cell of Leydig (IC) with blood vessel (Bv) in-between the seminiferous tubules. H and E, Scale bar = 50 μm

morphology as well as in cellular conformation occurred in 12 steps in this animal [Figure 2a-k]. The steps can be distributed among the four spermiogenic phases as follows: The first three steps [Figure 2a-c] constitute the *Golgi* phase; the *cap* phase consisted of the next three steps [Figure 2c-e]. While the next three steps [Figure 2f-h] make up the acrosomal phase, the last three steps [Figure 2i-k] constitute the *maturation* phase.

The three spermatids in the Golgi phase had spherical nuclei with varying chromatin distributions. In the newly formed spermatid after the second meiotic division, the chromatin in its round nucleus was distributed as irregular patches with thin peripheral layer [Figure 2a]. In the cytoplasm, which was apparently less electron dense, Golgi complexes were beginning to appear at the Golgi zone near the nucleus. The presence of roundish mitochondria, endoplasmic reticular cisternae, and ribosomal granules was also beginning to be apparent in the cytoplasm. In the Step 2 spermatids [Figure 2b], the round nuclei had irregularly dispersed chromatin with less at the periphery and the nuclear membrane tends to increase in thickness. In the cytoplasm, the proacrosomal granules began to transform into the acrosomal vesicle with the two parallel centrioles taking positions near the Golgi zone. There was also the presence of cisternae of endoplasmic reticulum, ribosomal granules, and numerous mitochondria that exhibit typical linear cristae.

In the 3rd step spermatid, the acrosomal granule attaches to the nuclear envelope with the development of the acrosomal vesicles [Figure 2c]. In the Step 4 spermatid [Figure 2c], acrosomal granule which is now closely attached to the nucleus exhibits a thickening at the area of contact and flattens over the nucleus without indenting it. At this step, the nucleus has irregularly dispersed chromatin.

The main feature of Step 5 and 6 spermatids was the formation of the acrosomal cap by the acrosomal vesicle

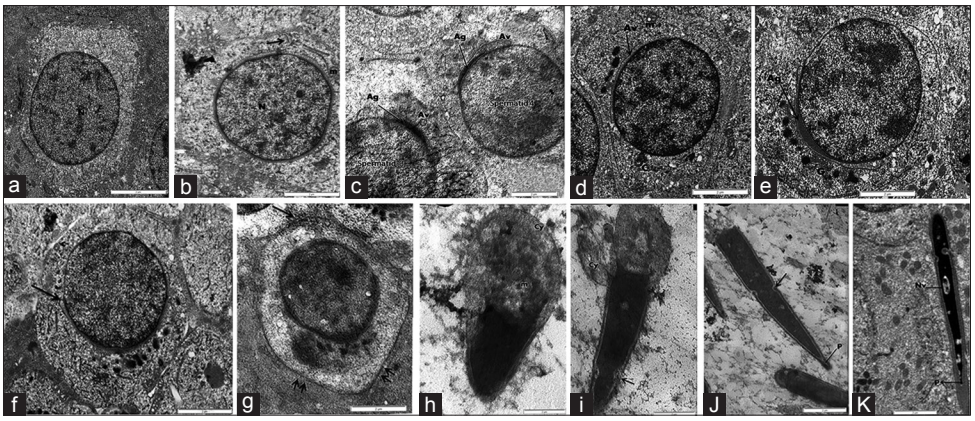

Figure 2: Electron micrographs of Step 1 and 2 spermatids in the greater cane rat. (a) Step 1-spermatid with spherical nucleus (N) having irregularly distributed chromatin patches. (b) Step 2-spermatid with the formation of the Golgi zone and acrosomal vesicles (arrow). Mitochondria (m) are also shown. Scale bar = 2 μm. (c) Electron micrographs of Steps 3 and 4 spermatids in the greater cane rat. Step 3-spermatid has the acrosomal granules (Ag) attached to the nucleus and the acrosomal cap (Av) formed on it while in Step 4-spermatid the attached acrosomal granule flattens over the nucleus and thickens at point of contact. Note in Spermatid 4, the flattening of the acrosomal vesicle, the irregularly distributed chromatin patches and the prominent nucleolus. Scale bar = 2 μm. Electron micrographs of Step 5 and 6 spermatids in the greater cane rat. In (d), Step 5-spermatid acrosomal vesicle (Av) spreads over the nucleus. Note the nuclear condensation and presence of mitochondria (m). In Step 6 spermatid (e), note the spreading over of the acrosomal granule (Ag) and the moving away of the Golgi from the acrosomal system. Scale bar = 2 μm. Electron micrographs of Steps 7 and 8 spermatids in the greater cane rat. (f) Step 7-spermatid has homologous acrosomal system with cap covering half of the nucleus. Note the marginal fossa (arrow) formed by the expanded cap margin and the location of the centriole (C). (g) Step 8-spermatid becoming elongated with acrosomal system moving close to the cell membrane (double arrows). Note the beginning of flagellar axoneme development (long arrow). Scale bar = 2 μm. Electron micrographs of Steps 9 and 10 spermatids in the greater cane rat. In Step 9-spermatid (h), the nucleus abuts the cell membrane and the cytoplasm (Cy) moves towards the lumen. Note the mitochondria (m) in the cytoplasm. In (i), Step 10-spermatid become elongated spermatid with cytoplasmic residue (Cy) still hanging on it. Note the marginal fossa (arrow). Scale bar = 2 μm. Electron micrographs of Steps 11 and 12 spermatids in the greater cane rat. In Step 11-spermatid (j), the perforatorium (P) develops. Note the marginal fossa (arrow). In (k), Step 12-spermatid shows the more conspicuous nuclear vacuole (Nv) and the perforatorium. Scale bar = 2 μm

spreading over the round nucleus [Figure 2d and e]. In the Step 5 spermatid, while the nucleus remains spherical, its chromatin begins condensation with the centrioles moving away from the acrosomal system [Figure 2d]. The spreading of the acrosomal cap continues in Step 6 spermatids with increasing accumulation of the mitochondria around the acrosomal area. The acrosomal granule also begins to spread over the nucleus in this step, and the Golgi complex begins to move away from the acrosomal system [Figure 2e]. The nucleus in this step remains round with increasing chromatin condensation [Figure 2e].

In the Step 7 spermatids [Figure 2f], the acrosomal cap had extended to cover half of the nucleus with the acrosomic granule spreading along thereby making the acrosomal system have a homologous appearance. The expanded margin of the acrosomal vesicle also indents the nucleus to form a marginal fossa. At the same time, the spheroidal nucleus begins to change with the head area becoming conical. The spermatids also became oriented with the acrosomal system towards the basement membrane. Several axonemal fibers begin to appear in the cytoplasm with the tubular centrioles at the point of formation of the tail. The Step 8 spermatids are characterized by increased nuclear elongation and condensation [Figure 2g] with the cytoplasm also becoming conical. The spermatid nucleus with its acrosomal system begins to migrate toward the periphery of the cell. The first evidence of a flagellar axoneme at the development becomes apparent at this step [Figure 2g].

As the dorsal elongation and nuclear condensation continue in the Step 9 spermatid, the acrosomal system connects the cell membrane. At the same time, the bulk of the cytoplasm flows towards the other pole of the cell where the flagellum develops [Figure 2h]. In this step, the cytoplasm contains mitochondria that tend to gather at the region of the future middle piece of the spermatozoon. As the nuclear elongation continues, the acrosomal cap also continues its posterior extension to the caudal end of the nuclei in these spermatids. The continued elongation and condensation gave the nuclei in the 10 step spermatid its elongated shape [Figure 2i]. In this spermatid, the expanded acrosomal cap margins become apparent moving posterior and forming marginal fossa as the nucleus elongates, while occasional small vacuoles begin to appear in the more dense and compact nuclei. The formation of the spermatic tail with axonemal fibers appears within the cytoplasmic residues still persisting in this step.

In the Step 11 spermatid, rostral acrosomal extension which involved the anterolateral regions of the acrosomal cap becomes visible [Figure 2j]. Between the inner border of the acrosome and the nuclear envelope, the perforatium, and the subacrosomal space are equally present. With nuclear elongation, the marginal fossa moves caudally, thereby demarcating the equatorial segment from the middle segment of the acrosomal cap. The nuclear vacuoles were also on the increase [Figure 2j]. In the 12 step spermatid, three distinct segments of the acrosomic cap can be clearly distinguished;

the apical segment projecting beyond the anterior margin of the nucleus; a main segment extending back over and beyond the anterior half of the nucleus; and a differentiating equatorial segment comprising the caudal portion of the nucleus [Figure 2k]. The nuclear vacuole became more pronounced as this step marks the point of spermiation.

Discussion

The general pattern of spermiogenesis is similar in all mammals, but there are species difference in the fine detailed acrosomal formation and the resultant final shape of the acrosome over the sperm head.[4,12] The understanding of these species peculiarities is the major criteria in identifying the stages of the seminiferous epithelium cycle and subsequently the evaluation of the reproductive efficiency.[4,7] This work outlines the peculiarity in acrosomal development which will serve as the basis for the characterization of the stages of spermatogenic cycle and evaluation of reproductive efficiency in the greater cane rat.

From the ultrastructural analysis, the spermatid differentiation and acrosomal formation occurred in 12 steps in the greater cane rat. The number of spermiogenic steps varies among mammals and has been found to be species specific.[12,13] There are 19 steps in the rat,[14] 18 in the squirrel (*Funambulus palmarum*),[15] 16 in both mouse[16] and hamster,[17,18] 15 in both Mongolian and desert gerbils,[5,19] 14 in the monkey (*Macaca arctoides*),[20] and 12 in the dog[21] and Viscacha (*Lagostomus maximus maximus*).[6] The number of steps observed in the cane rat is similar to what has been reported in viscacha which is another hystricomorphic rodent. In all studied species, the steps are derived based on the changing morphology of the spermatids nuclei until the final shape of the spermatozoa is attained.[2,4,6,8] These changes have been linked to the pattern of chromatin condensation which is intrinsic to each species.[4]

While the general events of the formation and development of the acrosomal system in the greater cane rat is similar to those described in other rodents it, however, has its species-specific characteristics. Whereas in most rodents,[3,5,6,18] the head of the early spermatid was covered by the acrosomal vesicle and not by the acrosomal granules, in the cane rat the entire acrosomal system comprising the vesicle and granule covers the head of the early spermatid. This is comparable only to that described in the golden hamster.[14] In the same vein, after the attachment of the acrosomal granules to the nucleus, the nuclear surface may become flattened or indented with the degree of indentation varying from one species to another.[5,6] Although the import of the degree of flatness or indentation is yet to fully known, it has been reported that the acrosome may greatly indent or flatten the nucleus after which the sperm head of each species attains its characteristic shape.[5] Therefore, the observed flattening of the nuclear surface by the acrosome with no clear indentation in the cane rat, contrary to what obtains in the rat,[14] Viscacha[6] and gerbil[5] but consistent with that in the monkey,[22] is critical in the determination of the final shape of the sperm head in the cane rat.

Another species-specific characteristic in the spermatid differentiation in the greater cane rat is the abundance of nuclear vacuoles at nuclear elongation and condensation phases. In most rodents, it is either absent as in gerbil[5] or where present; it is small and occasional as in rat, rabbit, and monkey.[22] The presence of a large amount of nuclear vacuoles during the nuclear condensation phase similar to that observed in the cane rat has, however, been reported only in the human spermatids.[23]

Conclusion

Although the functional relevance of these peculiar characteristics observed in the spermatid differentiation is yet unknown, this work has provided valuable information on the spermiogenic process that will further the knowledge of spermatogenesis, aid the understanding of acrosomal reaction and consequently the reproductive biology of the male greater cane rat.

Acknowledgments

This work was funded by University of Ibadan Senate Research Grant (SRG/FVM/2010/1b) and the Switzerland-South Africa Joint Research Programme. We acknowledge the technical assistances of Ms. Pamela Sharp and Hasiena Alli (University of the Witwatersrand, Johannesburg); Ms. E. van Wilpe (University of Pretoria, South Africa) and Mr. E. O. Anise (Federal University of Agriculture, Abeokuta, Ogun State).

Financial support and sponsorship

Nil.

Conflicts of interest

There are no conflicts of interest.

References

1. Comizzoli P, Mermillod P, Mauget R. Reproductive biotechnologies for endangered mammalian species. Reprod Nutr Dev 2000;40:493-504.
2. Costa GM, Leal MC, Ferreira CS, Guimarães DA. França LR. Duration of spermatogenesis and spermatogenic efficiency in 2 large neotropical rodent species: The agouti (*Dasyprocta leporina*) and paca (agouti paca). J Androl 2010;31:489-9.doi: 10.2164/jandrol.109.009787.
3. Hess RA. Quantitative and qualitative characteristics of the stages and transitions in the cycle of the rat seminiferous epithelium: Light microscopic observations of perfusion-fixed and plastic-embedded testes. Biol Reprod 1990;43:525-42.
4. Segatelli TM, França LR, Pinheiro PF, Alemida CC, Martinez M, Martinez FE, *et al.* Spermatogenic cycle length and spermatogenic efficiency in the gerbil (*Meriones unguiculatus*). J Androl 2004;25:872-80.
5. Segatelli TM, Almedia CC, Pinheiro PF, Martinez M, Padovani CR, Martinez FE, *et al.* Ultrastructural study of acrosome formation in mongolian gerbil (*Meriones unguiculatus*). Tissue Cell 2000;32:508-17.
6. Muñoz EM, Fogal T, Dominguez S, Scardapane L, Guzmán J, Cavicchia JC, *et al.* Stages of the cycle of the seminiferous epithelium of the viscacha (*Lagostomus maximus*). Anat Rec 1998;252:8-16.
7. Segatelli TM, Almeida CC, Pinheiro PF, Martinez M, Padovani CR, Martinez FE, *et al.* Kinetics of spermatogenesis in the mongolian gerbil (*Meriones unguiculatus*). Tissue Cell 2002;34:7-13.

8. França LR, Godinho CL. Testis morphometry, seminiferous epithelium cycle length, and daily sperm production in domestic cats (Felis catus). Biol Reprod 2003;68:1554-61.
9. Abdelmalik SW. Histological and ultrastructural changes in the adult male albino rat testes following chronic crude garlic consumption. Ann Anat 2011;193:134-41.
10. Addo PG, Awumbila B, Awotwi E, Ankrah N-A. Reproductive characteristics of the female grasscutter (*Thryonomys swinderianus*) and formulation of colony breeding strategies. Livest Res Rural Dev 2007;15:1-3.
11. Adu EK, Yeboah S. On the use of the perineal stain as an index of sexual maturity and breeding condition in the male greater cane rat, (*Thryonomys Swinderianus, Temminck)*. Trop Anim Health Prod 2003;35:433-9.
12. Russell LD, Ettlin RA, Hikim APS, Clegg ED. Histological and histopathological evaluation of the testis. Int. J. Androl. 1993;16: 83.
13. Clermont Y. Kinetics of spermatogenesis in mammals: Seminiferous epithelium cycle and spermatogonial renewal. Physiol Rev 1972;52:198-236.
14. Leblond CP, Clermont Y. Definition of the stages of the cycle of the seminiferous epithelium in the rat. Ann N Y Acad Sci 1952;55:548-73.
15. Patil SB, Saidapur SK. Kinetics of spermatogenesis in the wild squirrel *Funambulus palmarum* (Linnaeus). Acta Anat (Basel) 1991;141:352-63.
16. Oakberg EF. A description of spermiogenesis in the mouse and its use in analysis of the cycle of the seminiferous epithelium and germ cell renewal. Am J Anat 1956;99:391-413.
17. Oud JL, de Rooij DG. Spermatogenesis in the chinese hamster. Anat Rec 1977;187:113-24.
18. van Haaster LH, de Rooij DG. Spermatogenesis is accelerated in the immature djungarian and Chinese hamster and rat. Biol Reprod 1993;49:1229-35.
19. Saidapur SK, Kamath SR. Kinetics of spermatogenesis in the Indian desert gerbil, *Meriones hurrianae* (Jerdon): Seminiferous epithelial cycle, frequency of stages, spermatogonial renewal and germ cell degeneration. Ann Anat 1994;176:287-95.
20. Clermont Y, Antar M. Duration of the cycle of the seminiferous epithelium and the spermatogonial renewal in the monkey *Macaca arctoides*. Am J Anat 1973;136:153-65.
21. Foote RH, Swierstra EE, Hunt WL. Spermatogenesis in the dog. Anat Rec 1972;173:341-51.
22. Bedford JM, Nicander L. Ultrastructural changes in the acrosome and sperm membranes during maturation of spermatozoa in the testis and epididymis of the rabbit and monkey. J Anat 1971;108:527-43.
23. Gordon M. Localization of the 'apical body' in guinea-pig and human spermatozoa with phosphotungstic acid. J Reprod Fertil 1969;19:367-9.